IVEM Investigation of Defect Evolution in FCC Compositionally Complex Alloys under Dual-Beam Heavy-Ion Irradiation

Calvin Parkin - University of Wisconsin-Madison - cparkin@wisc.edu, caparki@sandia.gov

Conventional nuclear structural alloys degrade severely after hundreds of displacements per atom, inadequately meeting the needs of next-generation fast reactors and triggering an investigation of compositionally complex alloys (CCA). Preliminary studies have shown that these alloys exhibit excellent mechanical properties and irradiation tolerance at high-temperature, promoting their candidacy for cladding and duct applications [1-20]. To investigate the fundamental mechanisms underlying the radiation resistance of compositionally complex base matrices, *in situ* dual-beam irradiations were performed on $Cr_{18}Fe_{27}Mn_{27}Ni_{28}$ and $Cr_{15}Fe_{35}Mn_{15}Ni_{35}$ at two elevated temperatures. Bubble populations were characterized at various dpa steps and compared to less compositionally complex reference materials.

Experimental or Technical Approach

Electropolished discs of $Cr_{18}Fe_{27}Mn_{27}Ni_{28}$ and $Cr_{15}Fe_{35}Mn_{15}Ni_{35}$ were irradiated *in situ* using the 300 keV Hitachi-9000 TEM at the IVEM-Tandem facility at Argonne National Laboratory (ANL) using a 1 MeV Kr^{2+} and 16 keV He^{+} dual-ion beam with a He/dpa ratio of 0.75%/dpa. Alloy selection, fabrication, preparation, precharacterization, and stopping range of ions in matter (SRIM) software inputs are detailed in references [11] and [3]. Pure Ni and a single-phase $Fe_{56}Ni_{44}$ binary alloy were used for reference against the two FCC CCAs. Two irradiation temperatures were selected: 500°C and 600°C. All irradiations but one were performed up to 7 dpa, as estimated by IVEM-developed correlations between counts measured by a Faraday cup and both SRIM and Iradina calculations for the dpa through a 100 nm-thick specimen [21, 22]. The 500°C Ni irradiation was performed to 1 dpa with a He/dpa ratio of 1%/dpa, as detailed in reference [23]. Dpa profiles for combined and individual ion species and He implantation are

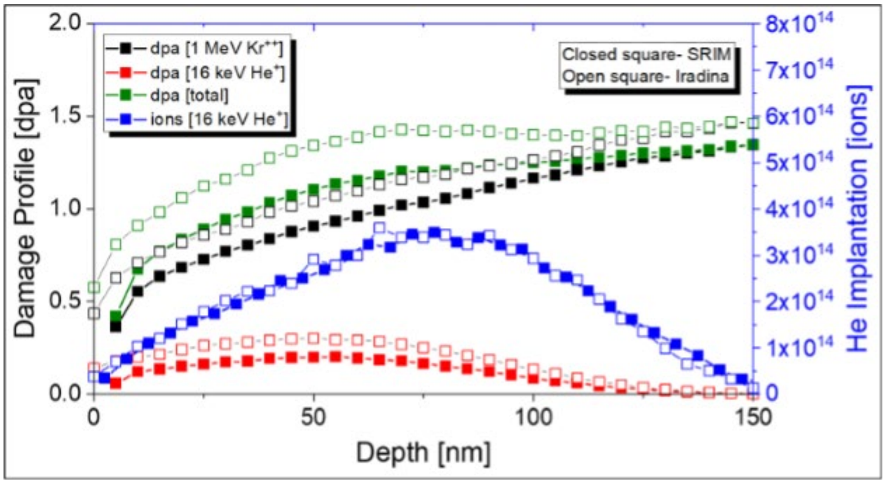

Figure 1. Kr^{2+} and He^{+} dpa and implantation profile for $Cr_{18}Fe_{27}Mn_{27}Ni_{28}$ generated by SRIM. Average of 1 dpa within first 100 nm. Kr^{2+} ions are high enough in energy to pass through the samples with minimal implantation.

shown in Figure 1. Bubble formation was confirmed using underfocused and overfocused conditions. Bubble diameters were measured using ImageJ software and used to calculate swelling levels. Lamellae thicknesses were measured by direct electron method (K2 camera) and a slit width of 15 eV.

Results

The bubble population for all materials at both temperatures at their final dpa is shown in Figure 2. The average bubble diameters, bubble number densities, and swelling levels are plotted in Figure 3. For each material, bubbles nucleate with higher density and with a smaller size at 500°C relative to 600°C, and the average diameter of bubbles remains higher at 600°C up to the maximum dpa. Due to the high density of bubble nucleation at 500°C, the swelling in $Cr_{18}Fe_{27}Mn_{27}Ni_{28}$ is slightly higher than at 600°C despite the limited bubble size (<2 nm diameter), which contrasts with the pure Ni and $Fe_{56}Ni_{44}$ binary alloy that exhibit significantly higher swelling at 600°C. The swelling levels in $Cr_{15}Fe_{35}Mn_{15}Ni_{35}$ at both temperatures are comparable; this indicates that although mobility is increased at 600°C, similar quantities of vacancies and interstitials can arrive at both bubbles and other sinks. Between the two temperatures, the bubble densities in $Cr_{15}Fe_{35}Mn_{15}Ni_{35}$ are closer together than were seen in $Cr_{18}Fe_{27}Mn_{27}Ni_{28}$, which demonstrates a reduced temperature effect on the mobility of vacancies and He atoms. Swelling levels in the two CCAs are consistently lower than the less compositionally complex materials.

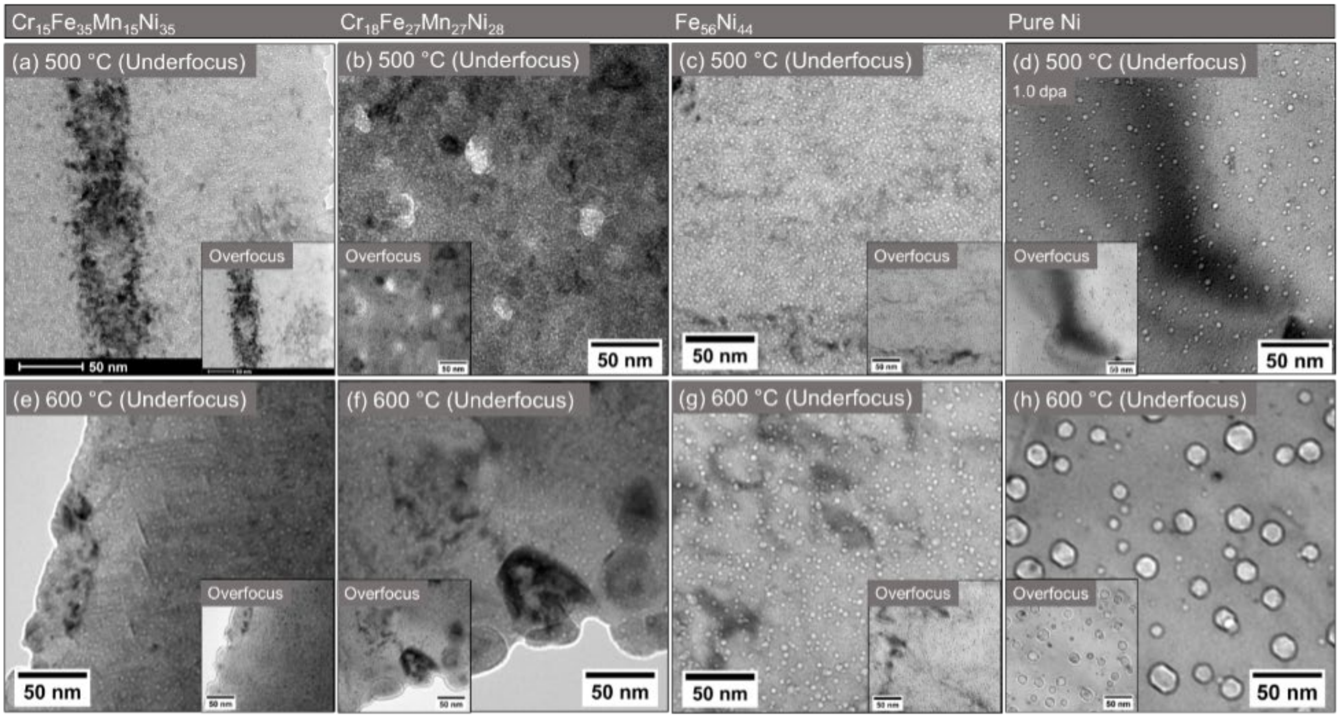

Figure 2. Bright-field micrographs of irradiated microstructures at final dpa of 1 dpa for pure Ni at 500°C [23] and 7 dpa for all other samples.

Discussion/Conclusion

Under favorable void-swelling conditions (i.e., dual-beam and high-temperature), bubbles nucleated in all irradiated materials. Under single-beam irradiation at 50 K, it was shown that $Cr_{18}Fe_{27}Mn_{27}Ni_{28}$ and $Cr_{15}Fe_{35}Mn_{15}Ni_{35}$ experienced a lower primary point defect production term than pure Ni and E90, a FeNiCr ternary alloy [11]. This reduction likely slowed bubble growth in CCAs compared to pure Ni and $Fe_{56}Ni_{44}$. Reference [23] proposed that vacancies generated in pure Ni under dual-beam conditions trap He atoms, leading to uniform nucleation of bubbles. In CCAs, the more localized and denser bubble nucleation is attributed to a distorted lattice, further trapping vacancies and He atoms.

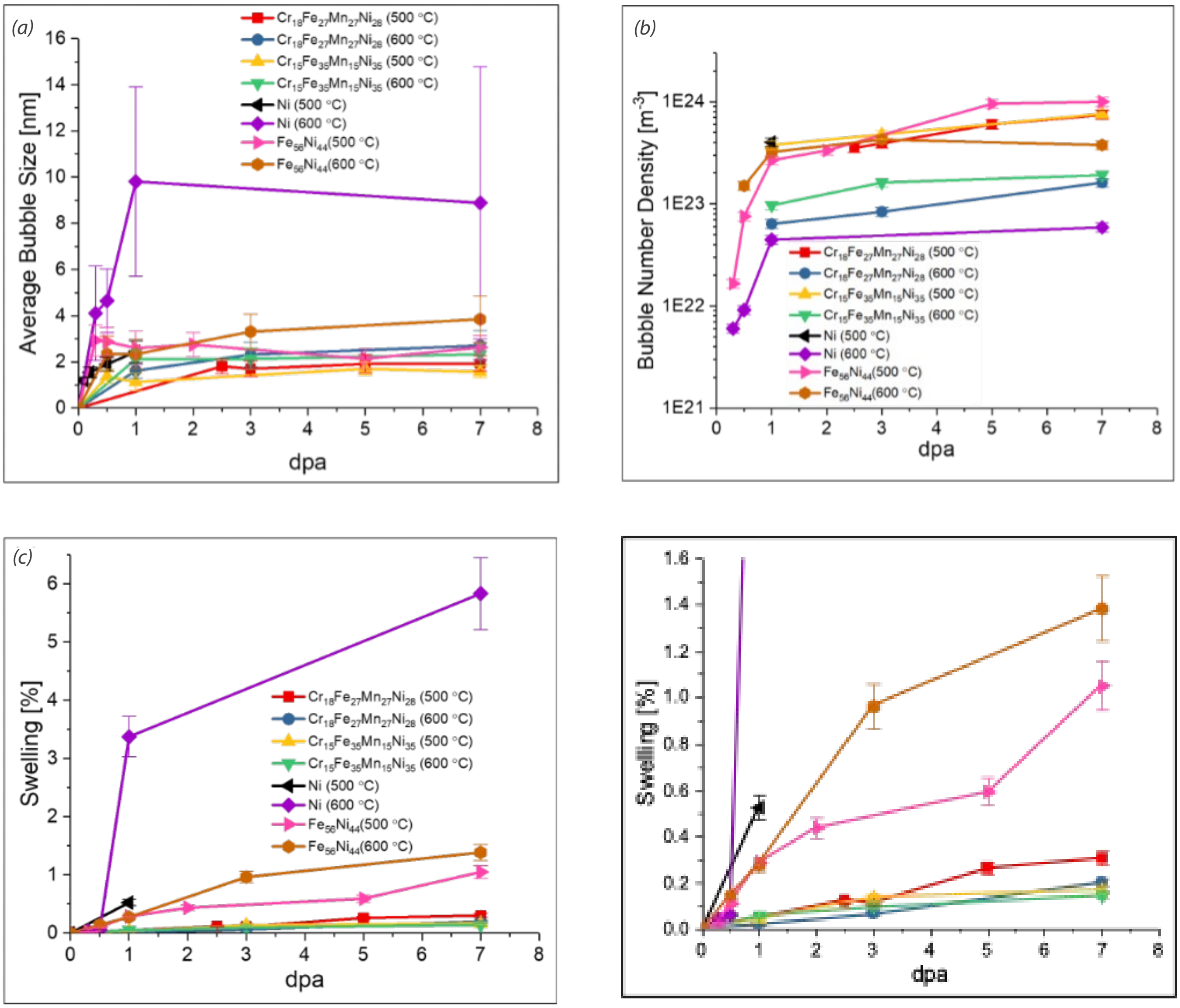

Figure 3. (a) Average diameter, (b) number density, and (c) calculated swelling of irradiated materials with zoomed in swelling axis on the right for clarity.

References

[1.] Miracle, D., and O. Senkov. 2017. "A Critical Review of High Entropy Alloys and Related Concepts." Acta Materialia 122: 448–511.

[2.] Kumar, N.A.P.K., et al. 2016. "Microstructural Stability And Mechanical Behavior of FeNiMnCr High Entropy Alloy under Ion Irradiation." Acta Materialia 113: 230–244.

[3.] Parkin, C., et al. 2022. "Phase Stability, Mechanical Properties, and Ion Irradiation Effects in Face-Centered Cubic FeCrMnNi Compositionally Complex Solid-Solution Alloys at High Temperatures." Journal of Nuclear Materials 565: 153733.

[4.] Egami, T., et al. 2013. "Irradiation Resistance of Multicomponent Alloys." Metallurgical and Materials Transactions A 45: 180–183.

[5.] Jin, K., et al. 2016. "Effects of Compositional Complexity on the Ion-Irradiation Induced Swelling and Hardening in Ni-Containing Equiatomic Alloys." Scripta Materialia 119: 65–70.

[6.] .Yang, T., et al. 2018. "Irradiation Responses and Defect Behavior of Single-Phase Concentrated Solid Solution Alloys." Journal of Materials Research 33 (19): 3077–3091.

[7.] Lu, C., et al. 2016. "Enhancing Radiation Tolerance by Controlling Defect Mobility and Migration Pathways in Multicomponent Single-Phase Alloys." Nature Communications 7: 13564.

[8.] Lu, C., et al. 2017. "Radiation-Induced Segregation on Defect Clusters in Single-Phase Concentrated Solid-Solution Alloys, Acta Materialia 127: 98–107.

[9.] Jin, K., and H. Bei. 2018. "Single-Phase Concentrated Solid-Solution Alloys: Bridging Intrinsic Transport Properties and Irradiation Resistance." Frontiers in Materials 5 (26).

[10.] Shi, S., et al. 2018. "Evolution of Ion Damage at 773K in Ni- Containing Concentrated Solid-Solution Alloys." Journal of Nuclear Materials 501: 132–142.

[11.] Parkin, C., et al. 2020. "In Situ Microstructural Evolution in Face-Centered and Body-Centered Cubic Complex Concentrated Solid-Solution Alloys under Heavy Ion Irradiation." Acta Materialia 198: 85–99.

[12.] Chen, W.-Y., et al. 2018. "Irradiation Effects in High Entropy Alloys and 316H Stainless Steel at 300°C." Journal of Nuclear Materials 510: 421–430.

[13.] Li, C., et al. 2019. "Neutron Irradiation Response of a Co-Free High Entropy Alloy." Journal of Nuclear Materials 527: 151838.

[14.] Egami, T., et al. 2015. "Local Electronic Effects and Irradiation Resistance in High-Entropy Alloys." The Journal of The Minerals, Metals & Materials Society 67 (10): 2345–2349.

[15.] Körmann, F., et al. 2017. "Phonon Broadening in High Entropy Alloys." Computational Materials Science 3.

[16.] Zhang, Y., et al. 2016. "Influence of Chemical Disorder on Energy Dissipation and Defect Evolution in Advanced Alloys." Journal of Materials Research 31 (16): 2363–2375.

[17.] Zhao, S., et al. 2019. "Frenkel Defect Recombination in Ni and Ni-Containing Concentrated Solid-Solution Alloys." Acta Materialia 173: 184–194.

[18.] Caro, M., et al. 2015. "Lattice Thermal Conductivity of Multi-Component Alloys." Journal of Alloys and Compounds 648: 408–413.

[19.] Béland, L., Y. Osetsky, and R. Stoller. 2016. "The Effect of Alloying Nickel with Iron on the Supersonic Ballistic Stage of High Energy Displacement Cascades." Acta Materialia 116: 136–142.

[20.] Zhang, Y., et al. 2015. "Influence of Chemical Disorder on Energy Dissipation and Defect Evolution in Concentrated Solid Solution Alloys." Nature Communications 6.

[21.] Stoller, R.E., et al. 2013. "On the Use of SRIM for Computing Radiation Damage Exposure."

[22.] Crocombette, J., and C.V. Wambeke, "Quick Calculation of Damage for Ion Irradiation: Implementation in Iradina and Comparisons to SRIM." EPJ Nuclear Sci. Technol. 5 (7) (2019).

[23.] Chen, W.Y., and M. Li. 2022. "Helium Bubble Formation in Nickel under In-Situ Krypton and Helium Ions Dual-Beam Irradiation." Journal of Nuclear Materials 558: 153342.

Publications

[1.] Parkin, C., et al. (under review)., "Microstructural Evolution of Compositionally Complex Solid-Solution Alloys under Dual-Beam Irradiation.", Acta Materialia.

Distributed Partnership at a Glance

NSUF Institution	Facilities and Capabilities
Argonne National Laboratory	Intermediate Voltage Electron Microscopy – Tandem Facility
Collaborators	
Argonne National Laboratory	Wei-Ying Chen (Co-Principal Investigator)
University of Wisconsin-Madison	Adrien Couet (Co-Principal Investigator)
Degrees Granted	
University of Wisconsin-Madison	Calvin Parkin, Ph.D.